Joint inversion of MT and CSEM data for Deep Mineral Exploration: Case Study of Koillismaa Layered Intrusion Complex

S. Védrine[1], C. Patzer[2], F. Bretaudeau[1], R., Rochlitz[3], U. Autio[2], B. Kim[1], F. Vermeersch[4], J. Kamm[2], C. Truffert[4], M. Darnet[1]
[1]BRGM, France, s.vedrine@brgm.fr, f.bretaudeau@brgm.fr, b.kim@brgm.fr, m.darnet@brgm.fr
[2]Geological Survey of Finland, Finland, cedric.patzer@gtk.fi, uula.autio@gtk.fi, jochen.kamm@gtk.fi
[3]Leibniz Institute for Applied Geophysics, Hanover, Germany, raphael.rochlitz@leibniz-liag.de
[4]IRIS Instruments, France, f.vermeersch@iris-instruments.com, c.truffert@iris-instruments.com

SUMMARY

A large-scale magnetotelluric (MT), controlled-source electromagnetic (CSEM), and deep induced polarization (IP) acquisition campaign was carried out around the Koillismaa Layered Intrusion Complex in northeastern Finland. The objective was to characterize deep-seated ultramafic intrusion with anomalous electrical and chargeability properties at approximately 1.4 km depth (as inferred by core values) and the associated alteration zones. MT is effective for targeting the deepest parts of the subsurface. However, its vertical resolution can be limited due to the plane wave nature of its sources. CSEM enhances and densifies data coverage by using a high number of powerful active current sources in the near field or transient zone of the receivers and by using less demanding measurement systems. Increasing transmitter (Tx) and receiver (Rx) points will, in turn, improve the vertical and lateral resolution at intermediate depths (< 3 km). In this paper, our goal is to present the key steps of combining MT and CSEM, encompassing survey design and logistics, data processing, and the final joint inversion. We display the isotropic resistivity models obtained from CSEM and MT individual inversions using a finite-element code. Additionally, we introduce the joint MT-CSEM inversion model, which merges the different sensitivities and resolutions of both methods and aligns with the expected geology of the area. Finally, we discuss future developments, such as exhaustive synthetic studies to validate our findings, IP effect correction or anisotropic inversions.

Keywords: Mineral, joint, CSEM, MT, IP

INTRODUCTION

The transition towards carbon neutral transportation and energy sources increases the global demand for mineral raw materials while easy-to-find near-surface (< 200 m) ore deposits are unlikely discovered in well-explored areas such as Europe. In order to increase the mineral exploration success rate, the project SEEMS DEEP (SEismic and ElectroMagnetic methodS for DEEP mineral exploration) develops geophysical deep exploration workflow capable of imaging the bedrock from the surface down to several kilometers depth. In this paper, we present a joint MT- CSEM inversion result from a survey conducted at the SEEMS DEEP geological test site (Figure 1), namely the Koillismaa Layered Intrusion Complex in north-eastern Finland. Here, a 1.7 km long hole drilled by GTK intersected mafic-ultramafic rocks with anomalous electrical and chargeability properties at 1.4 km depth, making it an interesting case study to test the ability of such technologies for imaging resistivity and chargeability contrasts at several kilometer depth.

METHODS

The survey design for MT, CSEM, and IP was based on both logistical constraints and theoretical considerations using various tools. Firstly, a 1D sensitivity test was conducted on a 200 m thick conductive layer at a depth of 1.5 km, evaluated against the level of noise measured in the field from a previous campaign for frequencies spanning from 32 s to 4096 Hz. The aim was to determine the maximum offset between Rx/Tx and the minimum source moment (in Ampere * dipole length) required to surpass the noise floor and detect the anomaly signature.

Once the maximum offset was determined (~ 15

km), 2D modeling was performed using MARE2DEM (Key 2016) and pyGIMLi (Rücker et al., 2017) on a synthetic model of the same conductive and chargeable body at a depth of 1.5 km. This analysis aimed to assess the response of the target in terms of amplitude, phase, and chargeability. Consequently, it helped to determine the optimum Tx orientations (cross-line or inline), frequency range selection, and Rx/Tx spacing to enhance sensitivity to the target while maintaining a reasonable number of Rx/Tx for a 3-week acquisition period. This encompassed the selection of the sampling frequency and operating time for MT recordings (preferably at late night when the signal is strongest in Finland), as well as waveform, duty-cycle, and fundamental frequency selection for CSEM.

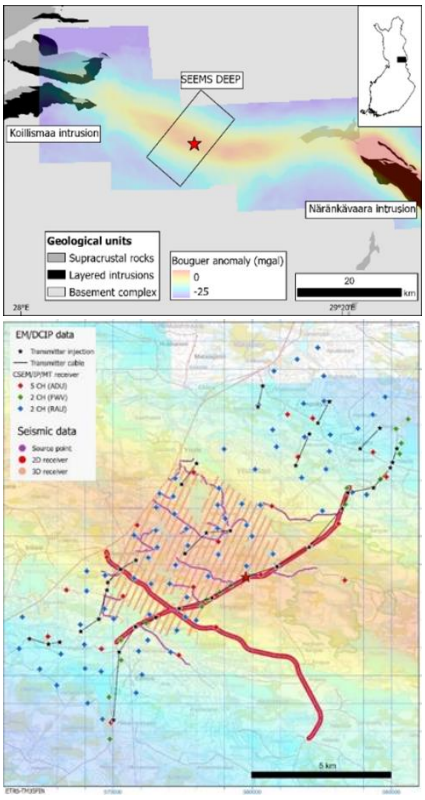

Figure 1. (a) Koillismaa Layered Intrusion Complex consists of Koillismaa and Näränkävaara intrusions and the unexposed source of the connecting gravity anomaly. The geological test area for SEEMS DEEP (black rectangle) is centred on the GTK deep drill hole (red star). **(b)** Layouts of 2D and 3D seismic surveys and EM receivers and sources for combined CSEM, MT and IP study.

Subsequently, 2D MARE2DEM inversions were conducted, including a mono-frequency CSEM inversion at 0.125 Hz mimicking Electrical Resistivity Tomography (ERT), a classic CSEM inversion spanning frequencies from 0.125 to 512 Hz, and an MT inversion. The purpose was to compare their ability to reconstruct the initial target in depth after data noise contamination. For this simplified case study with one body, it was concluded that MT imaging, without a dead-band and source effects, was the most suitable method for imaging such a target due to its higher sensitivity to conductors. Additionally, the multi-frequency CSEM inversion outperformed the mono-frequency inversion, attributed to the higher resolution provided by frequency sampling.

For the field data acquisition, we deployed 25 transmitter dipoles, each 1 km in length, and used three different galvanic transmitter systems (IRIS TIP 6000, Phoenix TXU-30, and Zonge GGT-3) capable of transmitting currents greater than a few Amperes in resistive grounds (> 1000 ohm-m), as found in such Archean basement rocks. CSEM waveforms consisted of square waves with fundamental frequencies ranging from 0.125 Hz to 512 Hz and a 50% duty cycle wave at 0.0625 Hz. Transmitted signal durations were chosen to ensure a minimum of 100 stacks at all frequencies. On the receiver side, we deployed 115 stations consisting of three types of systems: Metronix ADU08 MT recording electric and magnetic fields at 4096 Hz (+ 2 min of 65536 Hz), IRIS V-FullWaver recording electric fields at 100 Hz, and BRGM-made autonomous electric field stations based on Sercel RAU recording at 2000 Hz.

RESULTS

The CSEM data was obtained by extracting the Frequency-Domain Electromagnetic (FDEM) response from all electric field stations. To achieve this, we segmented all transmitter time series based on the start and stop times of each fundamental frequency of the square waves: 0.0625, 0.125, 0.5, 2, 8, 32, 128, and 512 Hz. Subsequently, for each receiver time series recorded within these intervals, we applied the frequency domain least-squares estimation algorithm implemented in the open-source code Razorback (Smaï and Wawrzyniak, 2020) to calculate the electric transfer functions and their error estimates at the fundamental frequency and 100 odd harmonics. A quality check was conducted to detect any outliers using a range of tools such as amplitude and phase spectra coherence, Argand diagrams, 1D inversions, and maps of the electric field vector orientations at receiver locations. Finally, synthetic data were computed using the semi-analytical code DIPOLE1D (Constable et al., 1987) within a synthetic 1D model derived from nearby resistivity core values. This synthetic data was compared to the measured field data from all transmitters, which allowed us to check the consistency of the measured field data in terms of amplitudes and

vector orientations with a 1D model response and to detect any reverse polarity in the transmitter signals or instrumentation mistakes made during receiver deployment.

The MT data was processed using GTK's robust processing code (m-estimator) to estimate the MT impedance tensors and their errors. At this stage, only ADUs' data were used in this study, although MT tensors were also estimated at each RAU electric field-only station using the closest magnetic recording as a reference. A quality check was then conducted by plotting apparent resistivity and phase soundings, mapping phase tensors, masking individual outliers, and performing 1D and 2D inversions to obtain a first approximation of the resistivity distribution in the area covered by the sites.

The QCed CSEM and MT data were inverted with isotropic conductivity individually and jointly in 3D using the open-source code custEM (Rochlitz et al., 2023), which relies on the inversion module pyGIMLi and employs the Gauss-Newton (GN) inversion scheme with Tikhonov regularization.

All inversions started from the same homogeneous 3D model of 10,000 ohm-m, using the same inversion grids and roughness parameters. The roughness parameter started at a fixed value at iteration 0 and decreased by a factor of 0.8 with each subsequent iteration. The accuracy of the custEM second-order finite-element forward modeling grid was validated against DIPOLE1D for our specific data geometry, and the relative error on the electric field magnitude was found less than 1% at receiver positions.

For the multi-frequency CSEM inversion, 51 receivers and 10 transmitters were used at frequencies of 0.125, 0.5, 2, 8, 32, 128, and 512 Hz, covering the entire spectrum. Both the real and imaginary parts of the two horizontal components of the electric field were inverted, with weights based on the inverse of standard errors estimated by the Razorback algorithm. A minimum error floor of 5% of the electric field magnitude was set to account for instrument errors.

For the MT inversion, 17 sites were used with each 43 frequencies evenly sampled between 2000 s and 1000 Hz. Both the real and imaginary parts of the four components of the MT tensors were inverted, with weights based on the inverse of standard errors estimated by the Razorback algorithm. A minimum error floor of 5% was set for Zxy and Zyx, while 30% was set for Zxx and Zyy.

Finally, a joint MT-CSEM inversion run was conducted using the same data, errors, and pyGIMLi setup as the individual inversions, without any weight adjustment at this stage.

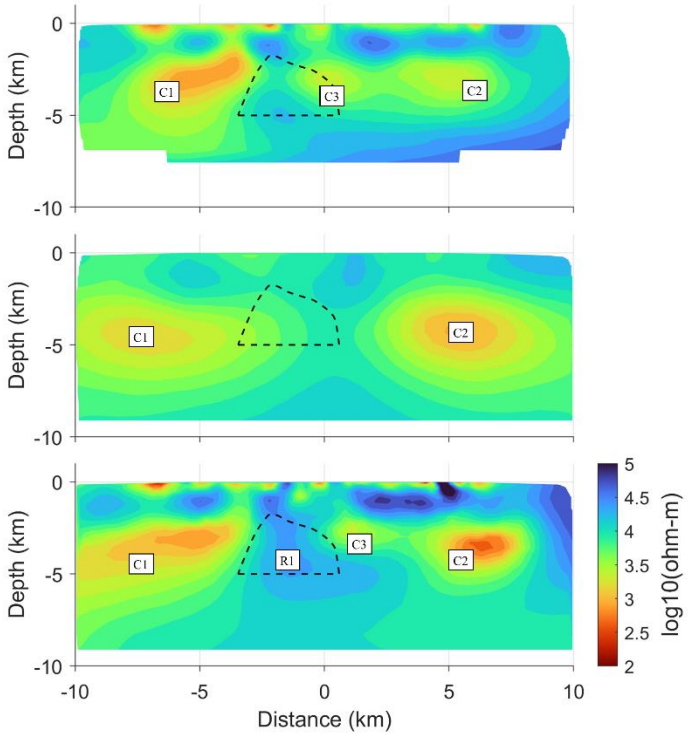

Figure 2. 3D inversion results - top: CSEM, middle: MT, bottom: MT-CSEM.

The CSEM residuals root mean square decreased from 17.55 to 1.50, MT from 20.48 to 1.10, and joint MT-CSEM from 14.57 to 1.10. Figure 2 displays the models in the same N45° oriented slice chosen to intersect the middle point of the 3D model, illustrating the varying resolutions of CSEM and MT. The MT model appears smooth, identifying two relatively conductive features labeled as C1 and C2. Conversely, the CSEM model exhibits roughness in the near-surface, highlighting conductive swamps (< 20 m depth) and resistive rocks (> 10,000 ohm-m between 1 and 3 km depth). Additionally, the CSEM model identifies the same conductors C1 and C2 at slightly different depths, along with an additional conductor, C3, in between.

Finally, the joint model, which fits both datasets equally, reveals an equivalent model that underscores the non-uniqueness problem inherent to electromagnetic methods. This model merges the vertical and lateral resolutions of CSEM at intermediate depth (< 3 km) with the MT model updates in the deepest part of the model (> 3 km). The approximate position of the ultramafic intrusion, inferred by legacy geophysical surveys including gravity and seismic profiles, is indicated by black dots. One can interpret that the joint inversion is better focusing the dense and resistive intrusion R1 to its expected position. However, further investigation is required as new 2D and 3D seismic

reflection data were acquired in the area.

Discussion

Efficient execution of the survey design is a key parameter for achieving a successful imaging. Logistical constraints are a top priority to address when conducting a grounded electromagnetic survey. These constraints include obtaining access permits from local administrations and private individuals, finding accessible roads or tracks for the Rx/Tx layout, finding favorable grounding points for current injection (conductive grounds), and avoiding cultural sources of noise such as pipes and power lines, which can affect or couple with our passive or active measurements, respectively. We also emphasize that the theoretical survey design is at least as important as logistics. It maximizes the sensitivity of the data geometry to the expected target while minimizing costs. Indeed, the number of Rx/Tx, the number of frequencies transmitted, the minimum stacks, and duty cycles can significantly increase or decrease acquisition time, necessitating to choose the best compromise between these parameters.

For the imaging part, thanks to the well-optimized custEM and its fine-element flexibility for refinement, we have been able to fit our datasets very accurately and obtain reliable isotropic resistivity models that were validated through post-inversion sensitivity tests. Although these preliminary results look promising for an isotropic joint MT-CSEM inversion and highlights the resolution improvement made by combining CSEM and MT, we intend to present a synthetic case study with the same data geometry to confirm the benefits of combining both methods while discarding uncertainties such as instrument noise or cultural noise. Additionally, we aim to address and invert IP effects influencing the CSEM data, and incorporate anisotropic inversion due to the layered structure of Archean gneiss.

Conclusions

The MT, CSEM, and IP survey design effectively balanced logistical constraints and theoretical considerations to optimize both the acquisition time (3-weeks) and the sensitivity of the data geometry to an expected target. Initial tests and 2D modeling and inversion guided the optimal setup for data acquisition. These tests on a simple synthetic case scenario showed that MT imaging was highly sensitive to a deep conductor, while multi-frequency CSEM provided higher resolution than ERT. Following the field survey, data processing utilizing Razorback and 3D inversions employing custEM highlighted the enhanced resolution achieved through joint MT-CSEM inversion, demonstrating the benefits of combining methods. Future work for electromagnetic will include synthetic case studies, IP correction, and anisotropic inversion to further validate and enhance the imaging process. At a larger scale, the next steps for the SEEMS DEEP project are to advance towards a multi-physics inversion that combines 3D electromagnetic, 2D/3D seismic reflection, gravity, and magnetic data.

Acknowledgements

SEEMS DEEP project has been funded through ERA-MIN3 Joint Call 2021. National funding agencies: Finland: Business Finland (640/31/2022), France: ANR (ANR-22-MIN3-0006-02), Sweden: VINNOVA, Poland: NCBR (ERA-MIN3/1/113/SEEMSDEEP/2022) The SEEMS DEEP field crew is thanked for their tremendous effort in acquiring the seismic and EM data sets. Seismic receivers by FLEX-EPOS seismic instrument pool (Research Council of Finland 328776) and electric field sensors from the Geophysical Instrument Pool Potsdam (GIPP) were used in SEEMS DEEP measurements. We would like to thank the CaSciModOT and CINES HPC facilities for providing the computing resources that made this work possible. Special thanks to the custEM development team for their availability and enriching discussions surrounding the code.

References

Constable, S.C., Parker, R.L., and Constable, C.G., 1987. Occam's inversion: A practical algorithm for generating smooth models from electromagnetic sounding data. Geophysics, 52(3), pp.289-300.

Key, K., 2016. MARE2DEM: a 2-D inversion code for controlled-source electromagnetic and magnetotelluric data. Geophysical Journal International, 207(1), pp.571-588.

Rochlitz, R., Becken, M., and Günther, T., 2023. Three-dimensional inversion of semi-airborne electromagnetic data with a second-order finite-element forward solver. Geophysical Journal International, 234(1), pp.528-545.

Rücker, C., Günther, T., and Wagner, F.M., 2017. pyGIMLi: An open-source library for modelling and inversion in geophysics. Computers and Geosciences, 109, pp.106-123. doi: 10.1016/j.cageo.2017.07.011.

Smaï, F., and Wawrzyniak, P., 2020. Razorback, an open-source Python library for robust processing of magnetotelluric data. Frontiers in Earth Science, 8, 296.